Preprints.org

Article

In-situ Evaluation of Different CAM Plants as Plant Microbial Fuel Cells for Recovery Energy in Atacama Desert

Felipe M. Galleguillos Madrid [*] , Norman Toro , Ingrid Jamett , Gilda Carrasco , Sergio Carvajal ,
Edward Fuentealba , Sebastián Salazar - Avalos , Douglas Olivares , Carlos Portillo , Alvaro Soliz ,
Luis Caceres , Mauricio Trigo

Article

In-situ Evaluation of Different CAM Plants as Plant Microbial Fuel Cells for Recovery Energy in Atacama Desert

**Felipe M. Galleguillos Madrid [1],*, Mauricio Trigo [1], Sebastián Salazar-Avalos [1],
Sergio Carvajal Funes [1], Douglas Olivares [1], Carlos Portillo [1], Edward Fuentealba [1],
Norman Toro [2], Gilda Carrasco S [3], Luis Cáceres [4], Ingrid Jamet [5] and Álvaro Soliz [6]**

[1] Centro de Desarrollo Energético de Antofagasta, Universidad de Antofagasta, Av. Universidad de Antofagasta 02800, Antofagasta 1271155, Chile; mauricio.trigo@uantof.cl (M.T.); sebastián.salazar@uantof.cl (S.S.A.); sergio_carvajal90@hotmail.com (S.C.F.); douglas.olivares@uantof.cl (D.O.); carlos.portillo@uantof.cl (C.P.); edward.fuentealba@uantof.cl (E.F.)

[2] Facultad de Ingeniería y Arquitectura, Universidad Arturo Prat, Iquique 1100000, Chile; notoro@unap.cl

[3] Department of Horticulture, Faculty of Agricultural Sciences, Universidad de Talca, Talca 3460000, Chile; gcarrasco@utalca.cl

[4] Departamento de Ingeniería Química y Procesos de Minerales, Universidad de Antofagasta, Av. Universidad de Antofagasta, Antofagasta 02800, Chile; luis.caceres@uantof.cl

[5] Centro de economía circular en procesos industriales, Universidad de Antofagasta, Av. Universidad de Antofagasta 02800, Antofagasta 127115, Chile; ingrid.jamett@uantof.cl

[6] Departamento de Ingeniería en Metalurgia, Universidad de Atacama, Av. Copayapu 485, Copiapó 1530000, Chile; alvaro.soliz@uda.cl

* Correspondence: felipe.galleguillos@uantof.cl; Tel.: +56-9-4235-2163

Abstract: Excess energy derived from photosynthesis can be used in plant microbial fuel cell (PMFC) systems as a sustainable alternative for electricity generation. In this study, the in-situ performance of CAM (Crassulacean Acid Metabolism) plants in Calama, Atacama Desert, was evaluated for energy recovery using PMFC with stainless steel AISI 316L and Cu as electrodes. The plant species evaluated included Aloe perfoliata, Cereus jamacaru, Austrocylindropuntia subulata, Agave potatorum, Malephora crocea, and Kalanchoe daigremontiana. Among the plant species, Kalanchoe daigremontiana demonstrated significant potential as an in situ PMFC, showing a maximum cell potential of 0.248 V and a minimum of 0.139 V. In addition, the cumulative energy for recovery was about 9.4 mWh m^{-2} of the electrode. The use of CAM plants in PMFC presents a novel approach to green energy generation, taking advantage of the inherent ability of these plants to adapt to arid environments and water-scarce areas such as Atacama Desert climate.

Keywords: plant microbial fuel cell (PMFC); CAM plant; Atacama Desert; solar energy; environmental engineering; sustainability

1. Introduction

The effect of climate change, pollution, and the depletion of natural resources, with the high percentage of the population living in areas with water scarcity (over 2.4 billion inhabitants), has led to the search for new forms of sustainable energy, such as photovoltaic systems [1] The recent trends worldwide are focused on developing technologies and innovations that allow the supply of energy to the population without generating a negative impact on the territory and environment. The Sun is the primary source of energy that supplies most of the processes on Earth and the Sun a year is greater than the total of all existing fossil energy resources on the planet. Despite this, there are still problems with making the most of solar resources, such as (i) the discontinuity of the resource and (ii) the high level of radiation dispersion, which generates a non-uniformity of the resource because of the movement of the Earth around the Sun. The reference data of solar radiation, which are the solar constant and the spectral distribution, are established for the average sun-earth distance conditions.

The solar constant is the energy that falls per unit area and per unit time on a surface normally oriented to the direction of propagation of solar radiation and located outside the Earth's atmosphere. This value varies slightly and is equivalent on average to 1367 W m^{-2}. [2,3] The radiation emitted by the Sun is distributed over a wide spectrum of wavelengths, with most of the radiated energy corresponding to the portion between 150 and 3000 nm, with a spectral distribution very similar to that produced by a black body at 5777 K. About half of this energy falls within the visible band, 390 to 770 nm. The rest corresponds almost entirely to infrared radiation, with a small percentage of ultraviolet radiation.

The Plant Microbial Fuel Cell (PMFC) uses plants and bacterial communities, principally the Geobacter genus, to generate electricity through natural processes that occur in the roots of plants. [4–11], One of the main challenges with the current state of technology is its power output. Even though the theoretical power output is estimated at 3.2 W m^{-2} in systems [12] with plants as the sole organic matter source [13–15]. The power yield of the PMFC can reach 1000 GJ ha^{-1}year^{-1} by considering a multidisciplinary European research consortium, and the hypothetical PMFC power yield of 21 GJ ha^{-1} year^{-1} is generally a traditional device [12]. When applied in an indigenous habitat, the power yield of PMFC is assessed to be limited to 1.6 MW km^{-2} [16]. While wind turbines and solar panels could create 5 to 7.7 MW km^{-2} and 4.5 to 7.5 MW km^{-2} respectively, on a typical windy day under Western European conditions [9].

Plants produce organic material from sunlight and environmental CO_2 through photosynthesis. About 70% of the organic material ends up in the soil as dead root debris, mucilage, and exudates [17–22]. The organic material that fixes the plants in the soil can be oxidized by the rhizosphere bacterial community's releases of CO_2, protons (H^+), and electrons (e^-). These e^- are donated by bacteria when operating their metabolic processes. The H^+ and dissolved O_2 are part of O_2 reduction reaction (ORR) mechanisms, generating electrical work during e^- reduction. [23,24]The PMFC device is considered a specific solar cell, transforming the biochemical energy to electricity under specific electrochemical work [16]. The materials used as electrodes have total relevance. Various materials, such as Cu, Ni, C (graphite), Ti, and among others, have been tested as anode materials because of their catalytic activity. [25,26] The Cu metal has the following characteristics, (i) it is known to be an antimicrobial material (Cu ions are toxic for the planktonic bacterial cells and prevent biofilm formation), (ii) the Cu conductivity is close to 900 times well than the polycrystalline graphite, (iii) decrease the internal resistance, and (iv) reduce the amount of required electrode material considerably [27–30]. The Cu corrosion products avert the creation of electrochemically active biofilms over the Cu anode electrode, especially during the start-up of the electrochemical period when biofilm formation still must take place, and the anode potential due to the missing reduction power of a fully established microbial biofilm may shift into the corrosion potential. [31,32] On the other hand, stainless steel AISI 316L materials are used as cathode electrodes with interesting performance [22,33]. The potential difference between the anode and cathode simplifies the movement of e^- by an external circuit to decrease an e^- acceptor such as O_2 at the cathode surface. [34,35] Using this renewable energy is an imperative need to develop agriculture even in the most desert-like climates with plants growing locally.

It is one of those rare studies to analyze the in-situ behavior of CAM plants for possible use as PMFC. This study is based on the extensive data obtained from the application of AISI 316 and Cu electrodes in different CAM plants that can grow at considering the following (i) high levels of solar radiation, (ii) tolerance to water stress, (ii) resistance to temperature variations present, and (iv) different open circuit potentials (OCP) behavior.

2. Materials and Methods

2.1. Open Circuit Potential (OCP) Monitoring.

The experimental procedure was designed to examine the potential (V) generation from in situ CAM plants in Calama located in Atacama Desert. The electrodes used were a Cu plate as an anode and an stainless steel AISI 316L plate as a cathode of 10 cm^2. The PMFC single chamber with electrodes thoughtfully positioned around the rhizosphere (1mm distance) represents a sophisticated

bioelectrochemical marvel. It ingeniously taps into the dynamic metabolic interplay of soil-dwelling microorganisms amidst plant roots to orchestrate a remarkable feat: the generation of electricity. This ingenious setup capitalizes on the intrinsic synergy between plant biology, microbial consortia, and conductive materials to efficient electron transfers, culminating in electric current. The rhizosphere, the bustling realm where plant roots and the soil meet, becomes a nexus of activity. The roots exude is used as a spread for the resident microorganisms located in the rhizosphere. These electrons, tiny messengers of potential energy, traverse the conductive material of the anode electrodes, forging an intimate connection between the living world below and the inanimate electrode realm above. The study was designed considering 2 stations of study in the Atacama Desert climate. The CAM species were selected for their characteristics such as resistance to high levels of solar radiation, tolerance to water stress, and resistance to sudden variations in temperature. All experiments used a data logger AEMC model L452 for continuously collecting OCP potential fluctuations. The PMFC was monitored for periods of 8 days on average. The recording intervals of the sampled information are every 1 second for the variables potential (V), temperature (°C), relative humidity (RH, %), and radiation (Wm^{-2}) using the horizontal global radiation.

2.2. Electrodes Surface Characterization.

The morphological analysis of the cathode and anode electrode surface was characterized by scanning electron microscopy (SEM), using a Hitachi SU 500 microscope.

2.3. Meteorology Monitoring.

The experiment was carried out in Calama (Figure 1). This city is located at 2260 m.a.s.l. in the Atacama Desert (22° 28′ 0″ S, 68° 55′ 60″ W). It presents a Köppen climate rating of type BWk', which corresponds to a cold arid zone (Figure 1a) [36]. It offers an excellent quality of solar resources which shows an average per day of 7.22 kWh m^{-2} of global horizontal irradiance (GHI), obtaining a total of 2,632 kWh m^{-2} annually. This zone is characterized by annual precipitation that does not exceed 50 mm year^{-1}, which is reflected in clear skies throughout the year, as shown in Figure 1b) (satellite image taken by MODIS-Terra, instrument from space, August 23rd, 2022) [37]. The atmospheric parameters involved in the study were evaluated with a meteorological station in the city. Ambient Temperature (Tamb) and relative Humidity (RH) were measured with a young thermometer and hygrometer models CS215-L11 and hmp60-L11, respectively. Global horizontal irradiance (GHI) was measured with a Kipp & Zonen CMP21 pyranometer. The resolution of each measured parameter was 1s and was recorded as an average value per minute.
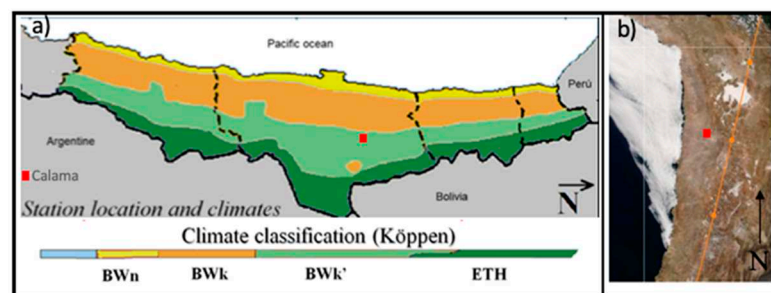

Figure 1. a) Calama location and climatic classification according to Köppen, Antofagasta Region, Chile. (Image based on Marzo et al.) [38], c) Picture was taken by MODIS-Terra instrument from space, on August 23th, 2022 (http://aeronet.gsfc.nasa.gov). The red square highlights the Calama location.

2.4. Experimental Data Analysis.

The model L452 datalogger records data by voltage (V) with a voltage range of 1V and an internal impedance of 1 MΩ (ref). The experimental data, for each test, were conducted between

06/07/2020 and 19/08/2020, with a sampling resolution of 1 minute. The cumulative energy generated by the plants needs the following sequence.

The current generated during the experiments was calculated using Ohm's law, according to the following expression.

$$I_p = \frac{V_p}{R} \; ; \tag{1}$$

where I_p is the current generated from the plants in A, V_p is the potential generated for the plants of the experimental measurements in V, and R is the impedance resistance of the equipment in Ω, respectively.

The power generated by the plants is calculated according to Equation 2.

$$P_p = V_p \cdot I_p; \tag{2}$$

where P_p is the power generated from the plants in W, V_p is the potential of the experimental measurements in V, and I_p is the current calculated using equation 1.

Finally, the accumulated energy recovery from the plant was obtained by calculating the area under the curve using the trapezoid method. according to the following expression.

$$E = \frac{(P_{p\_n} + P_{p\_n+1}) \cdot (t_{n+1} - t_n)}{2} \; ; \tag{3}$$

where E is the energy generate for each plant during the experiment in Wh, P_{p_n} is the power in W calculated using equation 2, t is the time in minutes, and n is the number of samples, respectively [39,40].

2.5. CAM Species Plants as PMFC.

The species used were seven and are (i) Aloe perfoliate [41,42], (ii) Cereus jamacaru [43–47], (iii) Austrocylindropuntia subulate [48–50], (iv) Agave potatorum [51–55], (v) Malephora crocea [56,57], (vi) Kalanchoe daigremontiana [58–63] and (vii) Aloe arborescens [64–66]. The soil used was a commercial composed of forest residues such as pine bark and sawdust and seaweed residues, with apparent density 0.4-0.7, pH (Dilution 1:5) 5-8.5, Electrical Conductivity (EC) Dilution 1:5) < 3 dS/m, C/N relation < 50 for each PMFC. The condition monitoring as climatic conditions was not controlled, being subjected to high or extreme levels of solar radiation, high temperature, and humidity relative fluctuations. The water supply to the system was controlled by watering the plants with only 100 ml every 7 seven days (before installing the electrodes) to generate a medium with high water stress.

3. Results and Discussion

The behavior of the open circuit potential (OCP, V) of the different PMFC concerning meteorological variables, such as (i) solar radiation, (ii) atmospheric humidity, and (iii) ambient temperature during a specific period are represented in Figures 2–4. Generally, the OCP performance of each PMFC presents a notable variability; however, they all present a cyclical behavior concerning the atmospheric variables analyzed in this study.
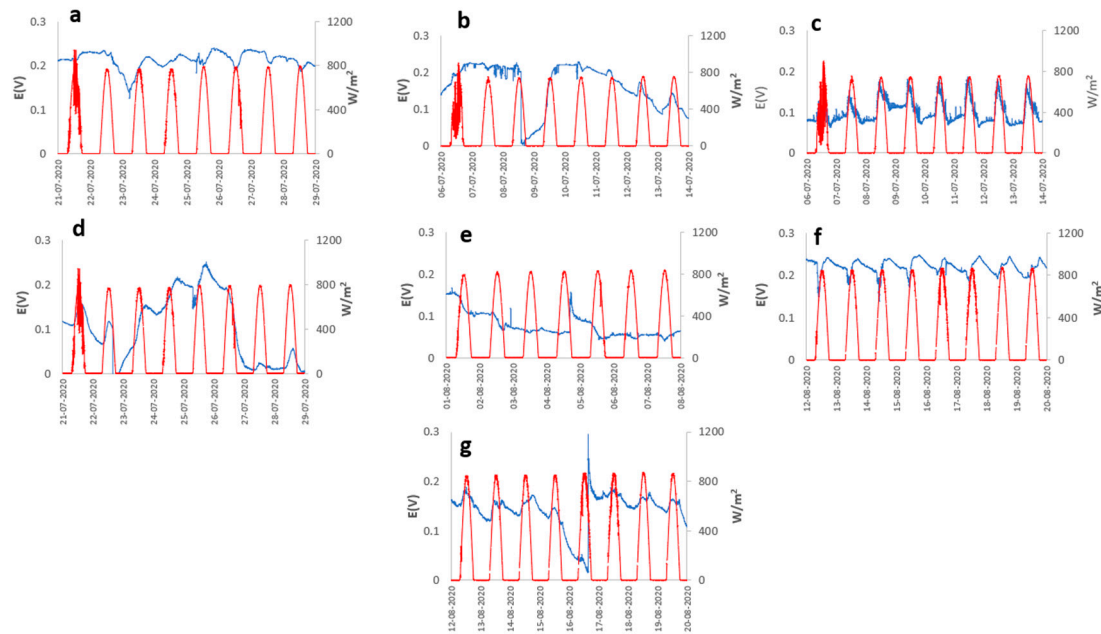
Figure 2. Potential (blue line) vs Solar radiation (red line) (a) Austrocylindropuntia subulata, (b) Aloe perfoliata, (c) Cereus jamacaru, (d) Malephora crocea, (e) Agave potatorum, (f) Kalanchoe daigremontiana, and (g) Aloe arborescens.

The species Cereus jamacaru and Kalanchoe daigremontiana represented in Figure 2c,f, respectively, show a notable cyclic behavior of the OCP concerning solar radiation, generating an OCP of 0.187 and 0.248V with a radiation level of 886.5 W m^{-2} and relative humidity in 8 days of analysis. The same cyclic behavior, despite not being so evident, is exhibited by Austrocylindropuntia subulata represented in Figure 2a, but from the second day of measurement, presenting its maximum OCP about 0.240 V in the periods of maximum solar radiation and relative humidity of about 942 W m^{-2} and 61% represented in Figure 3g. On the other hand, Aloe arborescens and Aloe perfolia represented in Figures 2g and 3b, show slight peaks in periods of higher solar radiation, generating a maximum OCP of 0.295V with solar radiation and an atmospheric humidity of 872 W m^{-2} and 54%, however, A. arborescens presents a more stable output potential compared to Aloe perfolia and the other species concerning time. Contrary to the previous cases, Malephora crocea and Agave potatorum represented in Figure 3d,e, do not show a good performance, however, their maximum OCP was 0.250 and 0.167V, respectively.
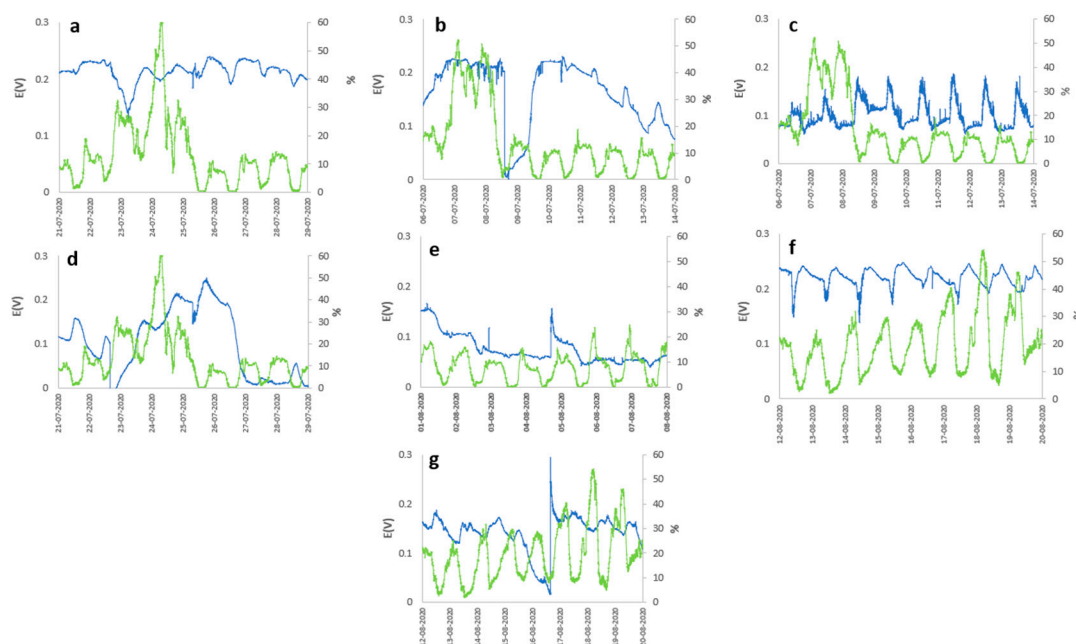
Figure 3. Potential (blue line) vs Atmospheric Humidity (green line) (a) Austrocylindropuntia subulata, (b) Aloe perfoliata, (c) Cereus jamacaru, (d) Malephora crocea, (e) Agave potatorum, (f) Kalanchoe daigremontiana, and (g) Aloe arborescens.

The behavior of PMFC concerning ambient temperature shown in Figure 4, generally maintains behaviors that are inversely proportional to humidity and directly proportional to solar radiation, so that in most cases, results like those from the analysis of radiation and humidity will be obtained. The performance for each of the seven plant species, even though not all of them behaved in the same way, is an expected result since they are different plant species with the same photosynthetic path. These will consist of a different rate of fixation of organic matter through its exudation in the rhizosphere, which will lead to variations in the colonies of electrogenic microorganisms.

The meteorological variables must play a fundamental role in the performance of the PMFC, as was observed in the results, in general, the majority of the plant species present a cyclical behavior of the generation of electrical energy, being directly related to the cycle of solar radiation from which two assumptions can be deduced, the first being that the performance is influenced by photosynthetic activity, produced by the greater activity of the stomata, which generates greater secretion of organic matter to the rhizodeposits, which triggers a greater activity of the rhizobacteria (responsible for generating electrical energy) due to an increase in the electrical interactions of the cell membrane as they have a greater amount of resources to metabolize. As a second assumption regarding the correlation of cell potential concerning meteorological variables, it consists of the availability of molecular O_2 in the cathodic zone that can be generated at times of greater solar radiation, which triggers an increase in ambient temperature (see Figure 4), which generates greater evaporation. of the substrate reducing humidity and a decrease in relative humidity that is related to the possible contribution of moisture to the substrate. This effect would trigger an increase in the efficiency in the anodic zone, since the greater the availability of O_2, the greater the rate of reduction of O_2 in H_2O, due to the effect of the ORR, with the $4e^-$ consume predominating direct formation of H_2O, compared to the $2e^-$ consume, which is less efficient and generates H_2O_2, which is harmful to microorganisms, which would affect the generation of electrical energy by reducing the microbial population of the electrochemical system.
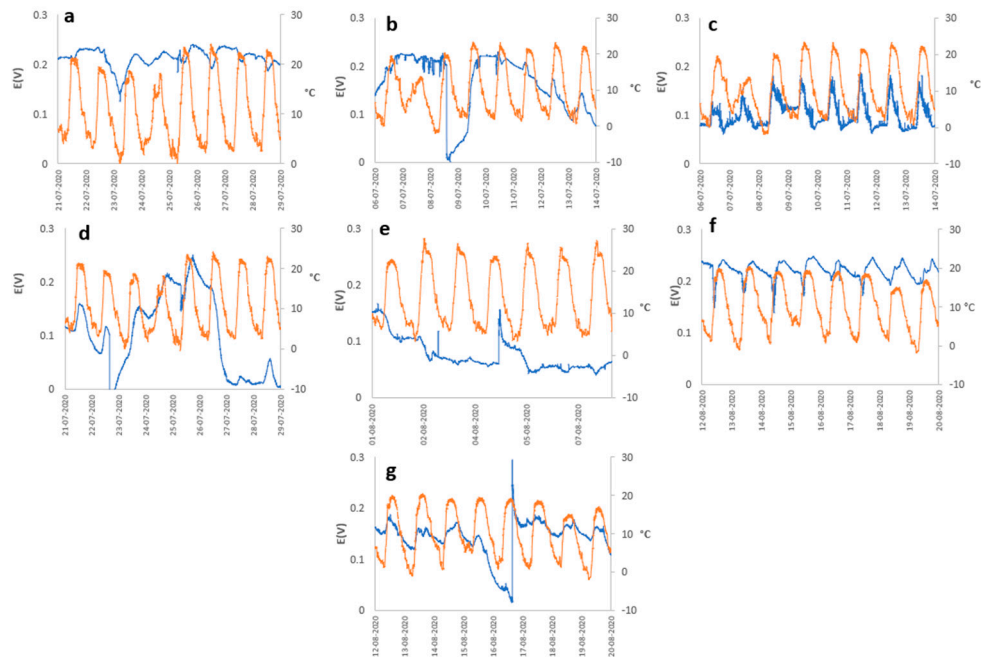
Figure 4. Potential (blue line) vs Ambient Temperature (orange line) (a) Austrocylindropuntia subulata, (b) Aloe perfoliata, (c) Cereus jamacaru, (d) Malephora crocea, (e) Agave potatorum, (f) Kalanchoe daigremontiana, and (g) Aloe arborescens.

Figure 5, illustrates the energy recovery performance of each plant concerning the prevailing environmental parameters, including solar radiation, relative humidity, and temperature according to equations 1 to 3. These graphs visually represent the correlation between these factors and the amount of energy harnessed by the plants through their microbial fuel cell systems. By examining the trends depicted in Figure 5, we can gain valuable insights into how variations in solar radiation, relative humidity, and temperature influence the overall energy generation potential of the plant microbial fuel cells. The data presented in this figure plays a crucial role in understanding and optimizing the efficiency of these sustainable energy conversion systems in diverse environmental conditions.
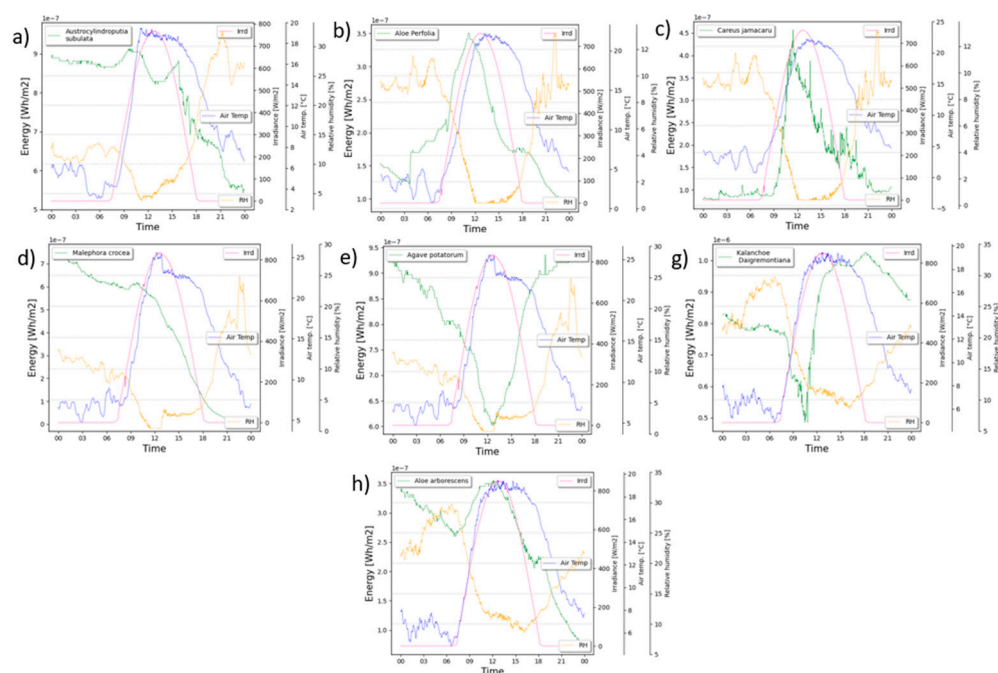
Figure 5. Energy generation performance per day in Wh m^{-2} of electrode; (a) Austrocylindropuntia subulata, (b) Aloe perfoliata, (c) Cereus jamacaru, (d) Malephora crocea, (e) Agave potatorum, (f) Kalanchoe daigremontiana, and (g) Aloe arborescens.

The experiment using CAM plants in PMFC yielded promising results, showcasing the energy recovery capabilities of each plant. The accumulated energy recovery values, measured in mWh m^{-2} of electrodes,: (i) Aloe perfoliata demonstrated an impressive energy generation of 5.9 mWh m^{-2}, (ii) Cereus jamacaru exhibited a respectable energy production of 2 mWh m^{-2}, (iii) Austrocylindropuntia subulata displayed a remarkable energy generation of 8.8 mWh m^{-2}, (iv) Agave potatorum demonstrated a noteworthy energy production of 7.8 mWh m^{-2}, (v) Malephora crocea showcased a considerable energy generation of 3.2 mWh m^{-2}, (vi) Kalanchoe daigremontiana displayed a significant energy production of 9.4 mWh m^{-2}, (vii) Aloe arborescens exhibited a commendable energy generation of 4.1 mWh m^{-2}. These energy recovery values demonstrate the potential of various CAM plants as efficient candidates for sustainable energy conversion in PMFC systems. The results offer valuable insights for optimizing and selecting suitable plant species to maximize energy generation in different environmental conditions, paving the way for eco-friendly and renewable energy solutions.
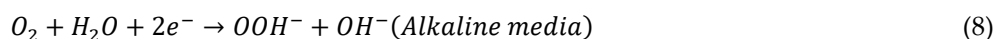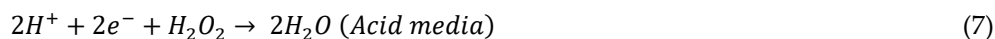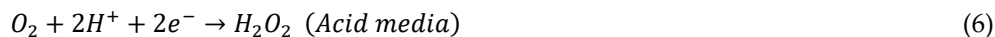
Plants have a characteristic that allows them to be grouped into three different types, depending on the environment in which they develop, they will have, to a greater or lesser extent, regulated something known as photorespiration, which is responsible for regulating the loss of water present in the plants. The photosynthetic pathways classifying into three classes: C3, C4, and CAM [56]. The plants in each class differ from each other. The efficiency of C4 plants in the photosynthesis process is higher than the other categories [21] reaching a maximum limit of 6% compared to C3 and 4.6% compared to CAM plants. They are the photosynthetic efficiency that defines the rate of conversion of solar energy into organic materials, thus allowing a greater proliferation of microorganisms. Understanding the photosynthetic pathways of plants is essential to choosing the right plant for the system. On the other hand, CAM plants that inhabit arid regions differ from C3 and C4 due to their ability to absorb CO_2 at night, leading to water conservation in their tissues. The CAM plants grow very slowly, resulting in lower biomass production than C3 and C4 plants. [67] Therefore, the choice of the type of plant will be even more relevant if it is to be used in places such as the north of Chile where radiation levels are very high, being around 1000-1300 W m^{-2} highlighting with violet colors the sectors of the Chilean territory with the highest rates of solar radiation. The CAM plants have adaptations to dry, arid climates. They use the Crassulacean Acid Metabolism (CAM) pathway to minimize photorespiration. The characteristic of this metabolic pathway is that instead of separating the light-dependent reactions and the use of CO_2 in the Calvin cycle, CAM plants separate these processes (CO_2 fixation) in time, which means that; during the night these plants open their stomata so that the CO_2 diffuses through the leaves and thus the CO_2 is fixed in the oxaloacetate by PEP carboxylase, the same step in the metabolism of the C4 and which is subsequently converted into malate or another organic acid. This acid is later stored in the vacuoles until the next day. The result of this process allows CAM plants to carry out photosynthesis during the day without the need to open their stomata. This product has organic acids stored in its vacuoles that decompose to release CO_2 and enter it into the Calvin cycle. Having controlled the release of CO_2 maintains a high concentration around the rubisco [17,24,56,67].

During the cathodic sub-process, the main e$^-$ acceptor is the dissolved O_2, which functions as a reductant and, in the presence of a suitable catalyst, can form H_2O. The process of e$^-$ acceptance and subsequent O_2 reduction is known as the oxygen reduction reaction (ORR) mechanism. This process can occur by the 4e$^-$ transfer process or by a 2e$^-$ transfer process, which will depend largely on factors such as the catalyst (cathode material) and the pH that will define the reaction path. Generally, there are two different pathways for the reaction of O_2 molecules; the first is the 4e$^-$ pathway, where O_2 is reduced directly into   two H_2O molecules in an acid medium or into four OH$^-$ molecules in a basic medium [7,68] as seen in the following reactions:

$$O_2 + 4H^+ + 4e^- \rightarrow 2H_2O \ \ (Acid\ media) \tag{4}$$

$$O_2 + 2H_2O + 4e^- \rightarrow 4OH^- \;\; (Alkaline \; or \; neutral \; media) \tag{5}$$

The second alternative for the reduction of the O_2 molecule is through the path of two e⁻, this is considered an incomplete process which occurs in two steps where O_2 is reduced to H_2O_2 in acid soil, in the case of the reduction of the O_2 molecule in alkaline medium is reduced to OH⁻, as shown below. [68]

$$O_2 + 2H^+ + 2e^- \rightarrow H_2O_2 \;\; (Acid \; media) \tag{6}$$

$$2H^+ + 2e^- + H_2O_2 \rightarrow 2H_2O \; (Acid \; media) \tag{7}$$

$$O_2 + H_2O + 2e^- \rightarrow OOH^- + OH^- (Alkaline \; media) \tag{8}$$

$$OOH^- + H_2O + 2e^- \rightarrow 3OH^- \; (Alkaline \; media) \tag{9}$$

The plant's main function is to provide nutrients to bacteria through photosynthetic reactions and generate an ideal space for the proliferation of bacterial colonies [69]. An unhealthy plant will have a lower yield, which means that it will run out of nutrients to feed the bacterial colonies present in the rhizosphere [70]. The PMFC (Figure 6) is based on the bioelectrochemical activity of microorganisms with the ability to degrade organic material and nutrients into simpler molecules such as CO_2 (metabolic waste) and also release e⁻ and H⁺, these processes occur in areas with high microbial activity and ideally with low levels of O_2, because the electrogenic bacteria (e⁻ donors) are mostly anaerobic and/or facultative bacteria, for this reason in the anodic zone (where the anodic electrode is located) is where the processes occur in their entirety capture and transfer of electrons that occurs when bacterial colonies form a biofilm on the anode surface, becoming electron donors, which is known as the process of extracellular electron transfer [71].

The anode in contact with the ground is populated with an electrogenic bacteria community concentrating these on its surface. The bacteria community releases e- during the metabolic process of nutrients present in the substrate creating a current circuit during the reduction process over the cathode surface. The reaction involved during the anodic sub-process is the following [72,73].

$$CH_3COO^- + 4H_2O \rightarrow 2HCO_3^- + 9H^+ + 8e^- \tag{10}$$
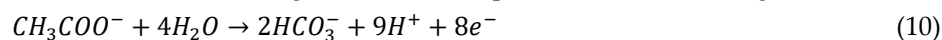
Figures 6, shows the anode electrode's morphological change during the electrochemical process before and after the bioprocess and contact this bacteria colony. Figure 6a indicates the electrode is pure Cu, and Figure 6c and 6e shows the result of an anodic subprocess where the dissolution of Cu is present as Cu → Cu²⁺ + 2e⁻ and the adhesion of nutrients such as Ca, Mg, C, K, and P and trace elements like Fe and Cu are evident over anodic electrode after bioprocess.
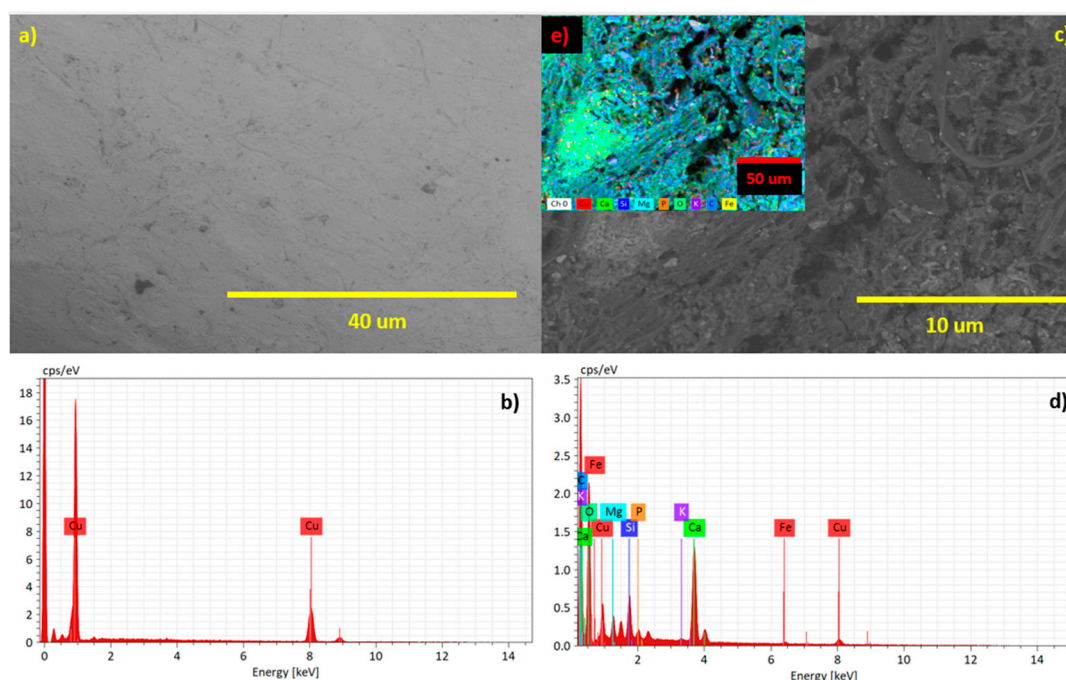
Figure 6. Surface morphology of the Cu anode electrode used for bioenergy recovery, a) Cu electrode before bioenergy recovery, c - e) Cu electrode after bioenergy recovery, b - d) XRD patterns of Cu electrode before bioenergy recovery with nutrient added over anode electrode.

The natural electron acceptors are oxygen, nitrogen, and sulfur, among others. [16] The great influencing factor on the efficiency and electricity production by the plant, are the climatic conditions, salinity of the soil, relative humidity, sun exposure time, radiation, and mainly the type of bacteria present in the piliferous zone of the root.

The e- transfer process occurs from proteins in the outer membrane via intracellular e- carriers such as $NAD^+/NADH$. This mechanism gives certain bacteria the ability to be the electrogenic process. The interaction that occurs between the e- donor and the electrode is known as extracellular electron transfer and occurs in three steps: (i) microbial oxidation (metabolic process), (ii) transfer from the intracellular carrier, and (iii) uptake from extracellular, respectively. In the area near the anode, oxidation reactions occur due to microbial activity. [74]Microorganisms can oxidize e- donors through a process called extracellular electron transfer. Therefore, this process involves both internal and external e- transport of the cell. Of which three transfer mechanisms are (i) direct e- transfer involving enzyme complexes associated or attached as a biofilm to the anode, (ii) indirect e- transfer, when a soluble organic or inorganic compound is oxidized in the cell and subsequently diffuses toward the acceptor (anode electrode), and (iii) direct transfer of e- through a conductive matrix in the form of pilus, called nanowires, respectively.

4. Conclusions

Based on the analysis conducted, CAM plants emerge as a promising and sustainable alternative for utilization in PMFC, particularly in regions characterized by high solar radiation and arid or hyper-arid climates such as the Atacama Desert in Northem Chile. The performance of PMFC employing CAM plants underscores the significance of nutrient availability, specifically Ca, Mg, C, K, and P, as well as trace elements like Fe and Cu, in optimizing electricity generation efficiency.

Among the CAM plants studied, Kalanchoe daigremontiana exhibits exceptional performance metrics. It demonstrates the highest electrical energy generation, remarkable consistency in cell potential, and minimal variations. This plant achieves a maximum cell potential of 0.248 V and a minimum of 0.139 V, with a recurrence rate of approximately 89% within the voltage range of 0.200 to 0.250 V. These results position Kalanchoe daigremontiana as a first candidate for further exploration on a larger scale due to its noteworthy attributes, including low variability in the open circuit potential (OCP). This low variability corresponds to a remarkable energy production of about 9.4 mWh m^{-2} of the electrode, further highlighting its viability for practical implementation. The energy estimate of energy generated by each CAM plant studied can be considered unique information which contributes to the scientific development of plant species adapted to desert climatic zones. However, while the potentials obtained from the metabolic processes of various CAM plant species exhibit relatively minor differences under the given conditions, determining the ultimate optimal species remains a challenge. Consequently, it becomes imperative to shift the focus of research toward the design and engineering of the electrochemical system itself. This approach aims to enhance energy recovery, thereby accommodating the extreme environmental conditions characteristic of the Atacama Desert, where this study was conducted.

Proposed avenues for further investigation involve the integration of soilless cultivation technologies within the context of the electrochemical system. This strategic approach is intended to provide insights into how CAM plants interact with the electrochemical environment when grown in controlled conditions, potentially yielding significant improvements in performance and energy output. In the context of the nutrient requirements for bacterial activity in the rhizosphere of these CAM plants within PMFC, it is important to acknowledge that the specific needs of bacteria can vary based on the particular bacterial species, the chosen plant species, and the composition of the soil. Furthermore, the availability of nutrients, including Ca, Mg, C, K, P, Fe, and Cu, is intrinsically linked to parameters such as pH, temperature, and humidity. These factors collectively influence the

microbial metabolic processes and the subsequent electricity generation in the PMFC systems. CAM plants, particularly exemplified by Kalanchoe daigremontiana, hold great promise as a sustainable solution for PMFC electrochemical systems in challenging environmental conditions. The study underscores the critical role of nutrients and trace elements in optimizing PMFC performance. Moving forward, a shift towards system-level design and engineering, coupled with controlled cultivation techniques, will be crucial for advancing the practical application of this innovative technology in extreme environments.

Author Contributions: Conceptualization: F.M.G.M, N.T, L.C., A.S, I.J. D.O, M.T, E.F, and C.P.; Methodology: F.M.G.M, L.C., M.T and D.O., Software, and validation: L.C, M.T, and F.M.G.M.; Formal analysis: F.M.G.M, S.S.A, and L.C.; Investigation: S.C, S.S.A, and F.M.G.M.; Resources: L.C, F.M.G.M, and E.F.; Data curation: F.M.G.M. S.C, and S.S.A.; writing—original draft preparation: F.M.G.M, L.C, N.T, G.C.S, A.S, M.T, and D.O.; writing—review and editing: F.M.G.M, L.C, N.T G.C.S., and E.F.; Supervision: F.M.G.M.; funding acquisition: F.M.G.M. All authors have read and agreed to the published version of the manuscript.

Data Availability Statement: The processed data are available from the corresponding author.

Conflicts of Interest: The authors declare no conflict of interest.

References

1. C. Parrado, A. Girard, F. Simon, and E. Fuentealba, "2050 LCOE (Levelized Cost of Energy) projection for a hybrid PV (photovoltaic)-CSP (concentrated solar power) plant in the Atacama Desert, Chile," *Energy*, vol. 94, pp. 422–430, 2016. https://doi.org/10.1016/j.energy.2015.11.015.
2. J. T. Kiehl and K. E. Trenberth, "Earth's Annual Global Mean Energy Budget."
3. D. Kim and V. Ramanathan, "Solar radiation budget and radiative forcing due to aerosols and clouds," *Journal of Geophysical Research Atmospheres*, vol. 113, no. 2, Jan. 2008. https://doi.org/10.1029/2007JD008434.
4. R. Nitisoravut and R. Regmi, "Plant microbial fuel cells: A promising biosystems engineering," *Renewable and Sustainable Energy Reviews*, vol. 76, no. September 2016, pp. 81–89, 2017. https://doi.org/10.1016/j.rser.2017.03.064.
5. L. De Schamphelaire *et al.*, "Microbial fuel cells generating electricity from rhizodeposits of rice plants," *Environ Sci Technol*, vol. 42, no. 8, pp. 3053–3058, 2008. https://doi.org/10.1021/es071938w.
6. K. Raman and J. C. W. Lan, "Performance and kinetic study of photo microbial fuel cells (PMFCs) with different electrode distances," *Appl Energy*, vol. 100, pp. 100–105, 2012. https://doi.org/10.1016/j.apenergy.2012.03.011.
7. K. Wetser, E. Sudirjo, C. J. N. Buisman, and D. P. B. T. B. Strik, "Electricity generation by a plant microbial fuel cell with an integrated oxygen reducing biocathode," *Appl Energy*, vol. 137, pp. 151–157, 2015. https://doi.org/10.1016/j.apenergy.2014.10.006.
8. R. A. Timmers *et al.*, "Microbial community structure elucidates performance of glyceria maxima plant microbial fuel cell," *Appl Microbiol Biotechnol*, vol. 94, no. 2, pp. 537–548, 2012. https://doi.org/10.1007/s00253-012-3894-6.
9. R. Shaikh *et al.*, "Bioelectricity production using plant-microbial fuel cell: Present state of art," *South African Journal of Botany*, vol. 140, pp. 393–408, 2021. https://doi.org/10.1016/j.sajb.2020.09.025.
10. A. Kouzuma, N. Kaku, and K. Watanabe, "Microbial electricity generation in rice paddy fields : recent advances and perspectives in rhizosphere microbial fuel cells," pp. 9521–9526, 2014. https://doi.org/10.1007/s00253-014-6138-0.
11. M. A. Moqsud, M. A. Hannan, and K. Omine, "Assessment of factors influencing bioelectricity generation in paddy plant microbial fuel cells," vol. 4, no. 12, pp. 840–850, 2015.
12. D. P. B. T. B. Strik, R. A. Timmers, M. Helder, K. J. J. Steinbusch, H. V. M. Hamelers, and C. J. N. Buisman, "Microbial solar cells: Applying photosynthetic and electrochemically active organisms," *Trends in Biotechnology*, vol. 29, no. 1. pp. 41–49, Jan. 2011. https://doi.org/10.1016/j.tibtech.2010.10.001.
13. M. Helder, D. P. Strik, H. V. M. Hamelers, and C. J. N. Buisman, "The flat-plate plant-microbial fuel cell : the effect of a new design on internal resistances The flat-plate plant-microbial fuel cell : the effect of a new design on internal resistances," 2012.
14. M. Helder, D. P. B. T. B. Strik, R. A. Timmers, S. M. T. Raes, H. V. M. Hamelers, and C. J. N. Buisman, "Resilience of roof-top Plant-Microbial Fuel Cells during Dutch winter," *Biomass Bioenergy*, vol. 51, no. 0, pp. 1–7, 2013. https://doi.org/10.1016/j.biombioe.2012.10.011.
15. M. Helder, D. PBTB Strik, H. V. Hamelers, and C. J. Buisman, "The flat-plate plant-microbial fuel cell: the effect of a new design on internal resistances," 2012. https://doi.org/10.1186/1754-6834-5-70.

16.   R. Shaikh *et al.*, "Bioelectricity production using plant-microbial fuel cell: Present state of art," *South African Journal of Botany*, vol. 140, pp. 393–408, Aug. 2021. https://doi.org/10.1016/j.sajb.2020.09.025.

17.   D. Brunelli, P. Tosato, and M. Rossi, "Flora Health Wireless Monitoring with Plant-Microbial Fuel Cell," *Procedia Eng*, vol. 168, pp. 1646–1650, 2016. https://doi.org/10.1016/j.proeng.2016.11.481.

18.   D. Brunelli, P. Tosato, and M. Rossi, "Flora monitoring with a plant-microbial fuel cell," in *Lecture Notes in Electrical Engineering*, Springer Verlag, 2017, pp. 41–48. https://doi.org/10.1007/978-3-319-55071-8_6.

19.   D. Brunelli, P. Tosato, and M. Rossi, "Microbial Fuel Cell as a Biosensor and a Power Source for Flora Health Monitoring."

20.   M. Helder, D. P. B. T. B. Strik, H. V. M. Hamelers, R. C. P. Kuijken, and C. J. N. Buisman, "Bioresource Technology New plant-growth medium for increased power output of the Plant-Microbial Fuel Cell," *Bioresour Technol*, vol. 104, pp. 417–423, 2012. https://doi.org/10.1016/j.biortech.2011.11.005.

21.   C. Wang, L. Guo, Y. Li, and Z. Wang, "Systematic Comparison of C3 and C4 Plants Based on Metabolic Network Analysis," *BMC Syst Biol*, vol. 6, no. SUPPL.2, 2012. https://doi.org/10.1186/1752-0509-6-S2-S9.

22.   S. Maddalwar, K. Kumar Nayak, M. Kumar, and L. Singh, "Plant microbial fuel cell: Opportunities, challenges, and prospects," *Bioresource Technology*, vol. 341. Elsevier Ltd, Dec. 01, 2021. https://doi.org/10.1016/j.biortech.2021.125772.

23.   M. Helder, D. P. B. T. B. Strik, H. V. M. Hamelers, R. C. P. Kuijken, and C. J. N. Buisman, "New plant-growth medium for increased power output of the Plant-Microbial Fuel Cell," *Bioresour Technol*, vol. 104, pp. 417–423, Jan. 2012. https://doi.org/10.1016/j.biortech.2011.11.005.

24.   R. A. Timmers, D. P. B. T. B. Strik, H. V. M. Hamelers, and C. J. N. Buisman, "Characterization of the internal resistance of a plant microbial fuel cell," *Electrochim Acta*, vol. 72, pp. 165–171, Jun. 2012. https://doi.org/10.1016/j.electacta.2012.04.023.

25.   C. C. Lin, C. H. Wei, C. I. Chen, C. J. Shieh, and Y. C. Liu, "Characteristics of the photosynthesis microbial fuel cell with a Spirulina platensis biofilm," *Bioresour Technol*, vol. 135, pp. 640–643, 2013. https://doi.org/10.1016/j.biortech.2012.09.138.

26.   S. Srikanth, T. Pavani, P. N. Sarma, and S. Venkata Mohan, "Synergistic interaction of biocatalyst with bio-anode as a function of electrode materials," *Int J Hydrogen Energy*, vol. 36, no. 3, pp. 2271–2280, Feb. 2011. https://doi.org/10.1016/j.ijhydene.2010.11.031.

27.   A. Baudler, M. Langner, C. Rohr, A. Greiner, and U. Schröder, "Metal–Polymer Hybrid Architectures as Novel Anode Platform for Microbial Electrochemical Technologies," *ChemSusChem*, vol. 10, no. 1, pp. 253–257, Jan. 2017. https://doi.org/10.1002/cssc.201600814.

28.   X. Qi, P. Liu, P. Liang, W. Hao, M. Li, and X. Huang, "Dual-signal-biosensor based on luminescent bacteria biofilm for real-time online alert of Cu(II) shock," *Biosens Bioelectron*, vol. 142, Oct. 2019. https://doi.org/10.1016/j.bios.2019.111500.

29.   Y. Zhang *et al.*, "Electrochemical and microbial community responses of electrochemically active biofilms to copper ions in bioelectrochemical systems," *Chemosphere*, vol. 196, pp. 377–385, Apr. 2018. https://doi.org/10.1016/j.chemosphere.2018.01.009.

30.   A. Baudler, I. Schmidt, M. Langner, A. Greiner, and U. Schröder, "Does it have to be carbon? Metal anodes in microbial fuel cells and related bioelectrochemical systems," *Energy Environ Sci*, vol. 8, no. 7, pp. 2048–2055, Jul. 2015. https://doi.org/10.1039/c5ee00866b.

31.   M. Asif *et al.*, "Unveiling microbiologically influenced corrosion engineering to transfigure damages into benefits: A textile sensor for H2O2 detection in clinical cancer tissues," *Chemical Engineering Journal*, vol. 427, Jan. 2022. https://doi.org/10.1016/j.cej.2021.131398.

32.   X. Zhu and B. E. Logan, "Copper anode corrosion affects power generation in microbial fuel cells," *Journal of Chemical Technology and Biotechnology*, vol. 89, no. 3, pp. 471–474, 2014. https://doi.org/10.1002/jctb.4156.

33.   K. R. S. Pamintuan and K. M. Sanchez, "Power generation in a plant-microbial fuel cell assembly with graphite and stainless steel electrodes growing Vigna Radiata," in *IOP Conference Series: Materials Science and Engineering*, IOP Publishing Ltd, Dec. 2019. https://doi.org/10.1088/1757-899X/703/1/012037.

34.   P. Bombelli *et al.*, "Comparison of power output by rice (Oryza sativa) and an associated weed (Echinochloa glabrescens) in vascular plant bio-photovoltaic (VP-BPV) systems," *Appl Microbiol Biotechnol*, vol. 97, no. 1, pp. 429–438, Jan. 2013. https://doi.org/10.1007/s00253-012-4473-6.

35.   D. R. Lovley, "Microbial fuel cells: novel microbial physiologies and engineering approaches," *Current Opinion in Biotechnology*, vol. 17, no. 3. pp. 327–332, Jun. 2006. https://doi.org/10.1016/j.copbio.2006.04.006.

36.   D. Watts, M. F. Valdés, D. Jara, and A. Watson, "Potential residential PV development in Chile: The effect of Net Metering and Net Billing schemes for grid-connected PV systems," *Renewable and Sustainable Energy Reviews*, vol. 41. Elsevier Ltd, pp. 1037–1051, Jan. 01, 2015. https://doi.org/10.1016/j.rser.2014.07.201.

37.   C. Herrera *et al.*, "Recharge and residence times of groundwater in hyper arid areas: The confined aquifer of Calama, Loa River Basin, Atacama Desert, Chile," *Science of the Total Environment*, vol. 752, Jan. 2021. https://doi.org/10.1016/j.scitotenv.2020.141847.

38.   A. Marzo *et al.*, "Sunbelt spectra comparison with standard ASTM G173: The Chilean case," in *AIP Conference Proceedings*, American Institute of Physics Inc., Nov. 2018. https://doi.org/10.1063/1.5067195.

39. M. Trigo-Gonzalez *et al.*, "Development and comparison of PV production estimation models for mc-Si technologies in Chile and Spain," *J Clean Prod*, vol. 281, Jan. 2021. https://doi.org/10.1016/j.jclepro.2020.125360.

40. M. Trigo-González *et al.*, "Hourly PV production estimation by means of an exportable multiple linear regression model," *Renew Energy*, vol. 135, pp. 303–312, May 2019. https://doi.org/10.1016/j.renene.2018.12.014.

41. S. M. Ezzat, A. M. El Sayed, and M. M. Salama, "Use of random amplified polymorphic DNA (RAPD) technique to study the genetic diversity of eight aloe species," *Planta Med*, vol. 82, no. 15, pp. 1381–1386, Apr. 2016. https://doi.org/10.1055/s-0042-108208.

42. A. J. Pegu and M. A. Sharma, "International Journal of Trend in Scientific Research and Development (IJTSRD) Review on Aloe Vera the Creative Commons Attribution License (CC BY 4.0)." [Online]. Available: http://creativecommons.org/licenses/by/4.0

43. V. Nessner Kavamura, R. G. Taketani, M. D. Lançoni, F. D. Andreote, R. Mendes, and I. Soares de Melo, "Water Regime Influences Bulk Soil and Rhizosphere of Cereus jamacaru Bacterial Communities in the Brazilian Caatinga Biome," *PLoS One*, vol. 8, no. 9, Sep. 2013. https://doi.org/10.1371/journal.pone.0073606.

44. J. C. Vencioneck Dutra *et al.*, "Cereus jamacaru D.C. hydroalcoholic extract promotes anti-cytotoxic and antitumor activity," *Pharmaceuticals*, vol. 11, no. 4, Dec. 2018. https://doi.org/10.3390/PH11040130.

45. N. Lídia *et al.*, "Seed reserve composition and mobilization during germination and early seedling establishment of Cereus jamacaru D.C. ssp. jamacaru (Cactaceae)," 2012. [Online]. Available: www.scielo.br/aabc

46. M. V. Meiado, L. S. C. De Albuquerque, E. A. Rocha, M. Rojas-Aréchiga, and I. R. Leal, "Seed germination responses of Cereus jamacaru DC. ssp. jamacaru (Cactaceae) to environmental factors," *Plant Species Biol*, vol. 25, no. 2, pp. 120–128, May 2010. https://doi.org/10.1111/j.1442-1984.2010.00274.x.

47. J. D. P. Bezerra *et al.*, "Fungal endophytes from cactus Cereus jamacaru in Brazilian tropical dry forest: A first study," *Symbiosis*, vol. 60, no. 2, pp. 53–63, Jun. 2013. https://doi.org/10.1007/s13199-013-0243-1.

48. S. A. Al-Robai, A. A. Ahmed, H. A. Mohamed, and F. O. Alzahrani, "Austrocylindropuntia subulata (Muehlenpf.) Backeb. (Cactaceae, Opuntioideae): an invasive new cactus record to the flora of Saudi Arabia," *Bioinvasions Rec*, vol. 11, no. 2, pp. 360–366, 2022. https://doi.org/10.3391/bir.2022.11.2.08.

49. W. El Bouaidi *et al.*, "Nature-based coagulants for drinking water treatment: An ecotoxicological overview," *Water Environment Research*, vol. 94, no. 8, Aug. 2022. https://doi.org/10.1002/wer.10782.

50. E. Basavand, P. Khodaygan, V. Babaeizad, H. Rahimian, and H. A. Mirhosseini, "Soft rot disease caused by Klebsiella aerogenes on Austrocylindropuntia subulata in Iran," *Indian Phytopathol*, vol. 73, no. 2, pp. 371–372, Jun. 2020. https://doi.org/10.1007/s42360-020-00201-6.

51. P. A. Santiago-García, E. Mellado-Mojica, F. M. León-Martínez, J. G. Dzul-Cauich, M. G. López, and M. I. García-Vieyra, "Fructans (agavins) from Agave angustifolia and Agave potatorum as fat replacement in yogurt: Effects on physicochemical, rheological, and sensory properties," *LWT*, vol. 140, Apr. 2021. https://doi.org/10.1016/j.lwt.2020.110846.

52. S. Rangel-Landa, A. Casas, and P. Dávila, "Facilitation of Agave potatorum: An ecological approach for assisted population recovery," *For Ecol Manage*, vol. 347, pp. 57–74, Jul. 2015. https://doi.org/10.1016/j.foreco.2015.03.003.

53. D. Soto-Castro, A. Pérez-Herrera, E. García-Sánchez, and P. A. Santiago-García, "Identification and Quantification of Bioactive Compounds in Agave potatorum Zucc. Leaves at Different Stages of Development and a Preliminary Biological Assay," *Waste Biomass Valorization*, vol. 12, no. 8, pp. 4537–4547, Aug. 2021. https://doi.org/10.1007/s12649-020-01329-2.

54. I. Torres, A. Casas, E. Vega, M. Martínez-Ramos, and A. Delgado-Lemus, "Population Dynamics and Sustainable Management of Mescal Agaves in Central Mexico: Agave potatorum in the Tehuacán-Cuicatlán Valley," *Econ Bot*, vol. 69, no. 1, pp. 26–41, 2015. https://doi.org/10.1007/s12231-014-9295-2.

55. X. Aguirre-Dugua and L. E. Eguiarte, "Genetic diversity, conservation and sustainable use of wild Agave cupreata and Agave potatorum extracted for mezcal production in Mexico," *J Arid Environ*, vol. 90, pp. 36–44, Mar. 2013. https://doi.org/10.1016/j.jaridenv.2012.10.018.

56. M. Veste and W. B. Herppich, "Comparative ecophysiology of the leaf-succulents Augea capensis (C3) and Malephora purpureo-crocea (CAM) in the Knersvlakte, Succulent Karoo, South Africa," *Flora: Morphology, Distribution, Functional Ecology of Plants*, vol. 278, May 2021. https://doi.org/10.1016/j.flora.2021.151807.

57. Arturo Goldarazena, Hugo Aguilar, Halil Kutuk, and Carl C. Childers, "Biology of three species of Agistemus (Acari: Stigmaeidae): life table parameters using eggs of Panonychus citri or pollen of Malephora crocea as food," *Exp Appl Acarol*, vol. 32, pp. 281–291, 2004. https://doi.org/10.1023/B:APPA.0000023247.69450.dc.

58. G. A. Molina *et al.*, "Green synthesis of Ag nanoflowers using Kalanchoe Daigremontiana extract for enhanced photocatalytic and antibacterial activities," *Colloids Surf B Biointerfaces*, vol. 180, pp. 141–149, Aug. 2019. https://doi.org/10.1016/j.colsurfb.2019.04.044.

59. C. van Maarseveen and R. Jetter, "Composition of the epicuticular and intracuticular wax layers on Kalanchoe daigremontiana (Hamet et Perr. de la Bathie) leaves," *Phytochemistry*, vol. 70, no. 7, pp. 899–906, May 2009. https://doi.org/10.1016/j.phytochem.2009.04.011.

60. J. Kolodziejczyk-Czepas *et al.*, "Antioxidant efficacy of Kalanchoe daigremontiana bufadienolide-rich fraction in blood plasma in vitro," *Pharm Biol*, vol. 54, no. 12, pp. 3182–3188, Dec. 2016. https://doi.org/10.1080/13880209.2016.1214740.

61. P. Domenico, "Effective microorganisms for germination and root growth in Kalanchoe daigremontiana," *World Journal of Advanced Research and Reviews*, no. 03, pp. 2581–9615, 2019. https://doi.org/10.30574/wjarr.

62. S. Von Caemmerer and H. Griffiths, "Stomatal responses to CO2 during a diel Crassulacean acid metabolism cycle in Kalanchoe daigremontiana and Kalanchoe pinnata," *Plant Cell Environ*, vol. 32, no. 5, pp. 567–576, May 2009. https://doi.org/10.1111/j.1365-3040.2009.01951.x.

63. U. Supratman, T. Fujita, K. Akiyama, and H. Hayashi, "Insecticidal compounds from Kalanchoe daigremontiana x tubiflora," *Phytochemistry*, vol. 58, pp. 311–314, 2001. https://doi.org/10.1016/S0031-9422(01)00199-6.

64. Y. Jia, G. Zhao, and J. Jia, "Preliminary evaluation: The effects of Aloe ferox Miller and Aloe arborescens Miller on wound healing," *J Ethnopharmacol*, vol. 120, no. 2, pp. 181–189, Nov. 2008. https://doi.org/10.1016/j.jep.2008.08.008.

65. F. Guillén *et al.*, "Aloe arborescens and Aloe vera gels as coatings in delaying postharvest ripening in peach and plum fruit," *Postharvest Biol Technol*, vol. 83, pp. 54–57, Sep. 2013. https://doi.org/10.1016/j.postharvbio.2013.03.011.

66. F. A. Andersen, "Final report on the safety assessment of aloe andongensis extract, aloe andongensis leaf juice, aloe arborescens leaf extract, aloe arborescens leaf juice, aloe arborescens leaf protoplasts, aloe barbadensis flower extract, aloe barbadensis leaf, aloe barbadensis leaf extract, aloe barbadensis leaf juice, aloe barbadensis leaf polysaccharides, aloe barbadensis leaf water, ferox leaf extract,...," *International Journal of Toxicology*, vol. 26, no. SUPPL. 2. pp. 1–50, 2007. https://doi.org/10.1080/10915810701351186.

67. S. Hartzell, M. S. Bartlett, and A. Porporato, "Unified representation of the C3, C4, and CAM photosynthetic pathways with the Photo3 model," *Ecol Modell*, vol. 384, 2018. https://doi.org/10.1016/j.ecolmodel.2018.06.012.

68. H. Yuan, Y. Hou, I. M. Abu-Reesh, J. Chen, and Z. He, "Oxygen reduction reaction catalysts used in microbial fuel cells for energy-efficient wastewater treatment: A review," *Materials Horizons*, vol. 3, no. 5. Royal Society of Chemistry, pp. 382–401, Sep. 01, 2016. https://doi.org/10.1039/c6mh00093b.

69. J. Wang *et al.*, "Bioenergy generation and rhizodegradation as affected by microbial community distribution in a coupled constructed wetland-microbial fuel cell system associated with three macrophytes," *Science of the Total Environment*, vol. 607–608, no. 2017, pp. 53–62, 2017. https://doi.org/10.1016/j.scitotenv.2017.06.243.

70. A. C. Sophia and S. Sreeja, "Green energy generation from plant microbial fuel cells (PMFC) using compost and a novel clay separator," *Sustainable Energy Technologies and Assessments*, vol. 21, pp. 59–66, 2017. https://doi.org/10.1016/j.seta.2017.05.001.

71. R. A. Timmers, D. P. B. T. B. Strik, C. Arampatzoglou, C. J. N. Buisman, and H. V. M. Hamelers, "Bioresource Technology Rhizosphere anode model explains high oxygen levels during operation of a Glyceria maxima PMFC," *Bioresour Technol*, vol. 108, pp. 60–67, 2012. https://doi.org/10.1016/j.biortech.2011.10.088.

72. A. A. Mier *et al.*, "A review of recent advances in electrode materials for emerging bioelectrochemical systems: From biofilm-bearing anodes to specialized cathodes," *Chemosphere*, vol. 283, Nov. 2021. https://doi.org/10.1016/j.chemosphere.2021.131138.

73. D. Akman, K. Cirik, S. Ozdemir, B. Ozkaya, and O. Cinar, "Bioelectricity generation in continuously-fed microbial fuel cell: Effects of anode electrode material and hydraulic retention time," *Bioresour Technol*, vol. 149, pp. 459–464, 2013. https://doi.org/10.1016/j.biortech.2013.09.102.

74. C. I. Torres, A. K. Marcus, P. Parameswaran, and B. E. Rittmann, "Kinetic experiments for evaluating the nernst-monod model for anode-respiring bacteria (ARB) in a biofilm anode," *Environ Sci Technol*, vol. 42, no. 17, 2008. https://doi.org/10.1021/es800970w.